Molecular-Scale Structure of the Cation Modified Muscovite Mica Basal Plane

ARTICLE *in* LANGMUIR · DECEMBER 1994

Impact Factor: 4.46 · DOI: 10.1021/la00024a028

6 AUTHORS, INCLUDING:

Simon Richard Biggs
University of Queensland
235 PUBLICATIONS **5,304** CITATIONS

SEE PROFILE

Peter J. Scales
University of Melbourne
193 PUBLICATIONS **3,908** CITATIONS

SEE PROFILE

Molecular-Scale Structure of the Cation Modified Muscovite Mica Basal Plane

S. Nishimura,[†,‡] S. Biggs,[†] P. J. Scales,[†] T. W. Healy,[*,†] K. Tsunematsu,[‡] and T. Tateyama[‡]

Advanced Mineral Products Research Centre, School of Chemistry, University of Melbourne, Parkville 3052, Australia, and Government Industrial Research Institute, Kyushu, Agency of Industrial Science & Technology (MITI), Shuku-machi, Tosu, Saga 841, Japan

Received November 12, 1993. In Final Form: April 18, 1994[⊗]

The muscovite mica basal plane surface was investigated directly with atomic force microscopy (AFM), zeta potential, and contact angle meausrements after H^+, Li^+, K^+, and Mg^{2+} ion exchange followed by heating at a temperature of 300 °C. Typical AFM images of the H- and K-mica showed an ideal array of light spots corresponding to one to five oxygen ions on the surface crystallographic layer of the muscovite mica. No spots were observed in the cavity surrounded by the light spots. In particular, the ideal image of H-mica, which should correspond to a bare basal plane where no interlayer cation exists, indicated that the calcination did not damage the mica basal plane. In the images of the Li- and Mg-micas, a significant irregular array of the light spots corresponding to the oxygen ions and small spots in the hexagonal cavity of the mica basal plane could be observed. Furthermore, the zeta potential of the H- and K-mica basal planes showed identical values to the freshly cleaved mica basal plane, while the zeta potential of Li- and Mg-mica basal planes were much lower in magnitude than freshly cleaved mica. These results substantiate that Li^+ and Mg^{2+} ions were irreversibly fixed in the hexagonal cavity on the mica basal plane, resulting in neutralization of negative charge. However, the K^+ ions could not be fixed in the hexagonal cavity. Such a cation-fixation process reflects the relative size of dehydrated cations and the size of the characteristic hexagonal cavity in the mica basal plane.

Introduction

The basal plane of muscovite mica has become the classic surface for solid–aqueous and solid–nonaqueous interfacial studies.[1–5] Such selection is predicted by the elegant atomically smooth array of oxygen atoms tetrahedrally coordinated to the silicon layer and in turn to the central octahedral aluminum layer.

Isomorphous substitution in the tetrahedral and octahedral layers leads to a net negative charge in the silicon–aluminum–silicon crystal layer, balanced, in the case of potassium mica, by interlayer K^+ ions.[6–8] The rigidity of the laminar structure and the large area over which chemical uniformity and atomic smoothness can be propogated are evident from many studies.

When swellable 2:1 type clay minerals (smectites) with small interlayer cations such as Li^+ and Mg^{2+} were heated at low temperatures around 200–300 °C, a loss of exchangeable cations and a reduction of layer charge were observed by Hofmann and Klemen[9] and Green-Kelly.[10–11] They postulated that this was due to the irreversible fixation of the small interlayer cations into the layered structure of these smectites. Despite widespread use of this effect in mineralogical studies, many questions still remain as to the mechanism of the fixation of small interlayer cations in smectites because of the small particle size and heterogeneous surface characteristics of clay mineral colloids.

To eliminate such complexities, our ongoing collaborative studies have focused on the pristine mica–electrolyte interface and thermally treated muscovite mica because it has both molecular homogeneity and an identical Si–O network to the clay basal plane.[7,8] In such thermally heated systems, freshly cleaved mica is exposed to various electrolyte (Li^+, K^+, or Mg^{2+} salt) solutions, removed, calcined at 300 °C, and washed and the subsequent solid–aqueous interface examined.

In the present study, we have selected atomic force microscopy (AFM), electrokinetic (zeta potential), and contact angle measurements to characterize the pristine and thermally heated mica basal plane–electrolyte interfaces.

The AFM has been used extensively to obtain topographical information at the angstrom resolution scale for molecular-scale observations on a variety of surfaces such as minerals, polymers, and biological materials.[12–14] In general, however, only very well ordered surfaces on the molecular scale have been successfully imaged. In a recent publication, it has been shown that true atomic resolution with the AFM may only be achieved at very low contact forces. These should typically be of the order of 10^{-11} N which approximates to the force between a single atom on the surface and a single atom on the scanning probe.[15]

Zeta potentials[16–18] and contact angles of mica basal planes were also measured before and after heat treatment

† University of Melbourne.
‡ Government Industrial Research Institute, Kyushu.
⊗ Abstract published in *Advance ACS Abstracts,* October 15, 1994.

(1) Israelachvili, J. N.; Adams, G. E. *J. Chem. Soc., Faraday Trans. 1* **1978**, *74*, 975.
(2) Pashley, R. M. *J. Colloid Interface Sci.* **1980**, *80*, 153.
(3) Pashley, R. M. *J. Colloid Interface Sci.* **1981**, *80*, 531.
(4) Christenson, H. K.; Horn, R. G. *Chem. Sci.* **1985**, *25*, 37.
(5) Christenson, H. K.; Gruen, D. W. R.; Horn, R. G.; Israelachvili, J. N. *J. Chem. Phys.* **1987**, *25*, 119.
(6) Radoslovich, E. W. *Acta Crystallogr.* **1960**, *13*, 919.
(7) Baily, S. W. In *Crystal Structure of Clay Minerals and their X-ray Identification*; Brindly, G. W., Brown G., Eds.; Mineralogical Society: London, 1980; Chapter 1.
(8) Baily, S. W. In *Review in Mineralogy*; Baily, S. W., Ed.; Mineralogical Society of America: Washington, DC, 1984; Volume 13 (MICAS).
(9) Hofmann, U.; Klemen, R. *Z. Anorg. Allg. Chem.* **1950**, *262*, 95.
(10) Green-Kelly, R. *Clay Miner. Bull.* **1953**, *2*, 52.
(11) Green-Kelly, R. *Mineral. Mag.* **1955**, *30*, 604.
(12) Binnig, G. *Ultramicroscopy* **1992**, *42–44*, 7.
(13) Marti, O.; Drake, B.; Hansma, P. K. *Appl. Phys. Lett.* **1987**, *51*, 484.
(14) Sarid, D. *Scanning Force Microscopy*; Oxford University Press: New York, 1991.
(15) Ohnesorge, F.; Binnig, G. *Science* **1993**, *260*, 1452.
(16) Scales, P. J.; Grieser, F.; Healy, T. W. *Langmuir* **1989**, *6*, 582.
(17) Nishimura, S.; Tateyama, H.; Tsunematsu, K.; Jinnai, K. *J. Colloid Interface Sci.* **1992**, *152*, 359.

0743-7463/94/2410-4554$04.50/0

using macroscopic mica sheets. Such techniques are capable of detecting small changes in surface charge and energy.

Experimental Section

Materials. Ruby muscovite mica, described previously,[8-10] from Bihar India was used in this present study. Prior to each experiment, the mica was carefully cleaved in air along the basal plane. To obtain a H^+-exchanged mica, freshly cleaved mica was repeatedly rinsed with water (pH 5.8) until the wash water conductivity after rinsing reached that of fresh water. The H^+-exchanged mica was immersed in 0.1 M LiCl, KCl, or $MgCl_2$ aqueous solutions for 12 h at ambient temperature to obtain Li^+-, K^+-, and Mg^{2+}-exchanged micas. After removal of the samples from the exchange solution, and without washing, these cation-exchanged micas were then calcined at 300 °C, followed by rinsing with water repeatedly until the water conductivity became equal to that of the fresh water. These exchanged-calcined samples are referred to as H, Li, K and Mg-micas, respectively. The water used in all experiments was prepared by distillation followed by percolation through charcoal and mixed bed ion-exchanged resins (Milli-Q water, $<5 \times 10^{-7}$ S cm^{-1}). All electrolytes were analytical grade reagents and were used as received.

Atomic Force Microscope. A Digital Instruments Nano-Scope III atomic force microscope (AFM) was used to observe the atomic structure of the mica basal plane. All images were obtained by using microfabricated silicon nitride cantilevers (Digital Instruments) with a manufacturers quoted spring constant of 0.58 N/m. We have independently calibrated these cantilevers and have found the spring constant to be 0.32 ± 0.02 N/m. The instrument was used in the constant deflection mode (i.e. tip−sample distance is adjusted to maintain a constant force and hence deflection of the cantilever). The reported images were recorded under water at ambient temperature and conditions using the AFM-A scanner which has a 1 μm × 1 μm scan range. Scanning forces were adjusted, under these conditions, to range from 10 to 100 pN. Molecular scale images were obtained without further filtering, although to enhance their effect, and to clarify the images, some of the presented data, as indicated, was filtered to remove high-frequency noise.

In a typical imaging experiment, a preprepared mica sample was mounted onto a steel puck using double sided tape before being put onto the top of the piezo scanner. The AFM head unit was then placed onto the mica sample after first mounting the scanning tip into the liquid cell. After sealing with an O-ring, water was introduced into the cell via a syringe. The tip and sample were then brought into contact and the imaging force adjusted to the desired strength for that experiment, typically around 10−50 pN. After adjustment of the imaging force, images were collected at scan rates of between 5 and 20 Hz, the speed being varied to gain the clearest images. The quality and reproducibility of all images were verified by changing parameters such as the scan size and direction while verifying that visible structures altered accordingly. In all cases, the images were also verified by scanning different areas of each sample, as well as two or more examples of each type of mica sample. All the images presented here are typical examples for that particular type of mica. The most important parameter for obtaining reproducible images was found to be the imaging force which must always be adjusted to a similar value to achieve similar images for the same samples.

The horizontal scan distances were calibrated by imaging a freshly cleaved mica plane at a resolution where the repeat unit cells, of five oxygens, were easily visible in the raw image. The nearest neighbor center−center separations of these unit cells are well defined and were used as the calibration distances.

Zeta Potential Measurement. The zeta potential of the mica basal plane was measured by the plane interface technique.[17] In this technique, the zeta potential was calculated from the Helmholtz−Smoluchowski equation using the electroosmotic mobility at the mica basal plane−aqueous solution interface. The procedure involves the analysis of the parabolic flow profile produced by electroosmosis in a rectangular cell with asymmetric interfaces, i.e., mica basal plane− and silica−aqueous solution interfaces. The parabolic flow profile of electrosmosis in the rectangular cell was obtained by measuring the mobilities of probe particles as a function of the cell depth.

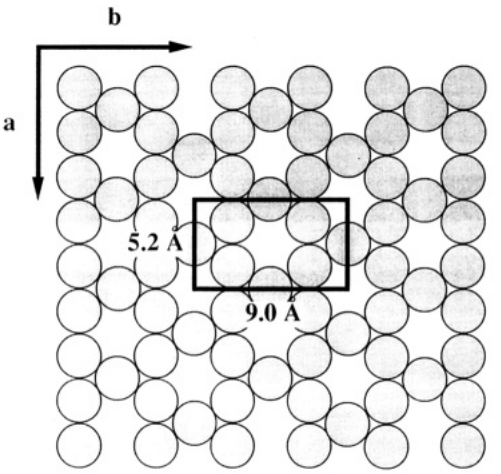

Figure 1. Molecular arrangement of oxygen ions on the basal plane of 2:1 type sheet silicates.

Contact Angle Measurement. The contact angles were measured at ambient temperature by the sessile-drop technique in a system isolated from vibration.[19,20] A mica sheet (10 × 10 mm) was placed in the measuring cell which was sealed from laboratory atmosphere and contained a reservoir of water to avoid evarporation. The profiles of sessile drops were monitored with a video camera and contact angles were determined by the tangent to the drop at the line of three-phase contact.

Results and Discussion

The hexagonal array of oxygen ions in the silicate layer of the basal plane of 2:1 type sheet silicates such as micas and smectites is shown diagrammatically in Figure 1. The unit cell used for calibration of the scanner is shown as a rectangle with dimensions of $a = 5.2$ Å and $b = 9.0$ Å.[21] The diameters for oxygen ions and for the cavity in a hexagonal ring are 2.8 and 2.6 Å, respectively.[22] All AFM images presented here will be discussed with reference to Figure 1.

The AFM images of the mica basal planes, which were calcined at 300 °C after ion exchange, are shown in Figures 2−5. The height scale used in Figures 2−5 corresponds to a range of 8−10 Å. The reality of all the images was verified each time by altering various parameters such as the scan size, scan rate, and direction of scan. If the images were seen to scale with scan size and the position of atomic features were seen to vary correctly with changes in the other scan parameters, then the images were considered to be real. The scanning forces employed were adjusted using the so-called "force mode", in the Nanoscope software, such that they were always in the range 10−100 pN. At these scanning forces the tip should interact with the surface with one or at the most a few atoms.[15] This is considered to be the prerequisite for true atomic or molecular scale images.

Figure 2a shows a raw top-view image of H-mica which should be equivalent to a bare mica basal plane in which any interlayer cations such as K^+ are removed. The high

(18) Nishimura, S.; Tateyama, H.; Tsunematsu, K. *J. Colloid Interface Sci.* **1993**, *159*, 198.

(19) Lamb, R. N.; Furlong, D. N. *J. Chem. Soc., Faraday Trans. 1* **1982**, *78*, 61.

(20) Scales, P. J.; Grieser, F.; Furlong, D. N.; Healy, T. W. *Colloids Surf.* **1986**, *21*, 55.

(21) Brindley, G. W.; Brown, G. *Crystal Structure of Clay Minerals and Their X-ray Identification*; Mineralogical Society: London, 1980; 495 pp.

(22) Spoisto, G. *The Surface Chemistry of Soil*; Oxford University Press: New York, 1984; 234 pp.

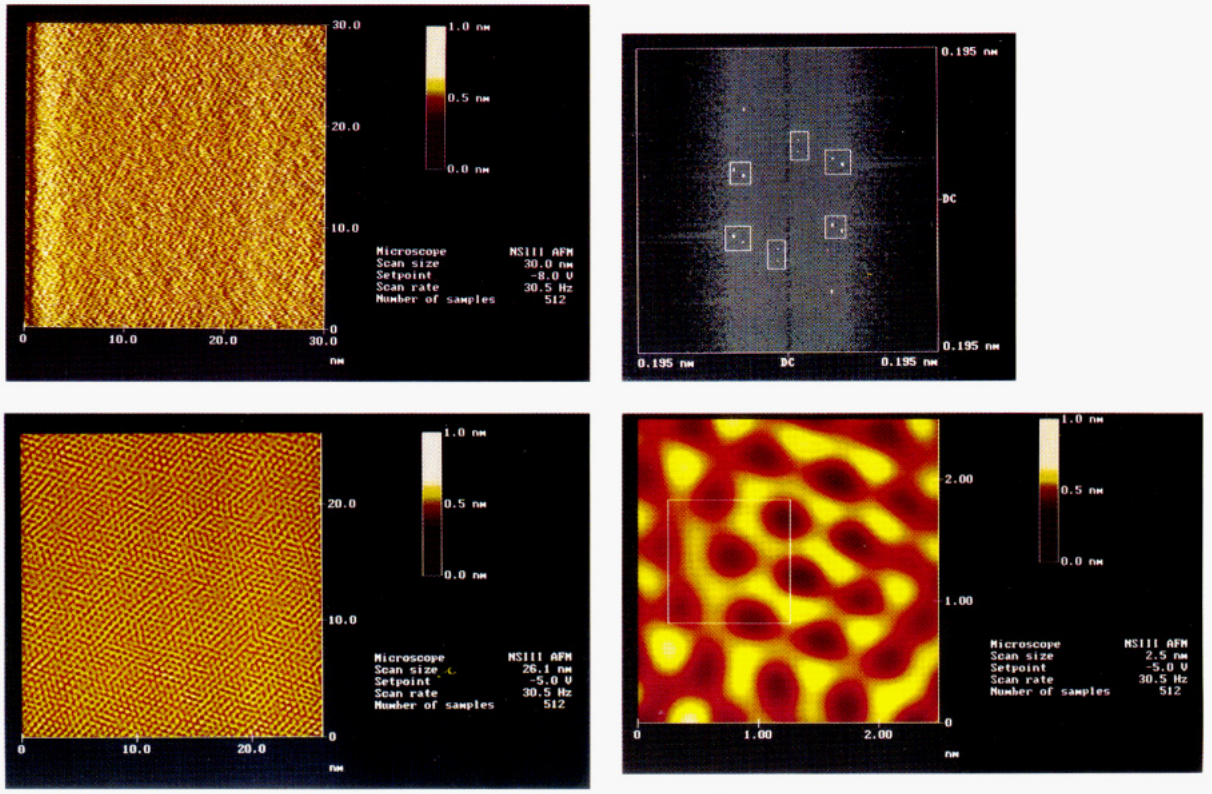

Figure 2. AFM images of a thermally treated H-muscovite mica basal plane: (a, top left) 30 nm × 30 nm unfiltered top view image; (b, top right) the 2-D fast Fourier transform of this raw image; (c, bottom left) a 26 nm × 26 nm high-frequency filtered image; (d, bottom right) a 3 nm × 3 nm close up image of the distortion present in the hexagons of oxygen ions seen in the previous image. The white box is used to highlight the distorted hexagon.

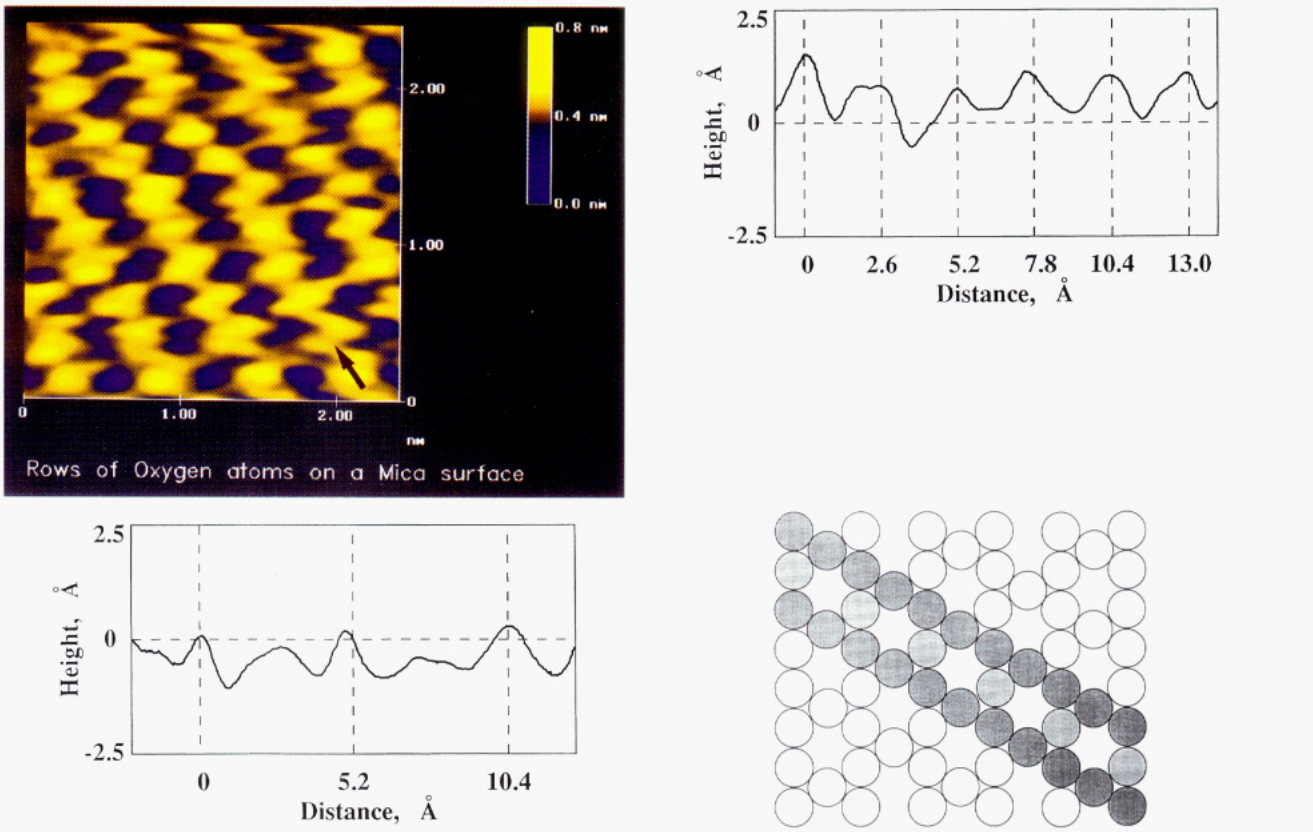

Figure 3. AFM image of a thermally treated K-muscovite mics basal plane: (a, top left) a 2.5 nm × 2.5 nm top view image; (b, top right) a section analysis of a close-packed row of light spots; (c, bottom left) a section analysis of a row of faint spots; (d, bottom right) the corresponding schematic arrays of oxygen ions.

degree of ordering in this image is easily apparent, the presence of hexagons of oxygen atoms being clearly visible. The 2-D Fourier transform of the raw data is shown in Figure 2b, where the hexagonal array of bright spots is indicative of the strong symmetric ordering in this raw image of the mica with a lattice spacing of about 2.6 Å.

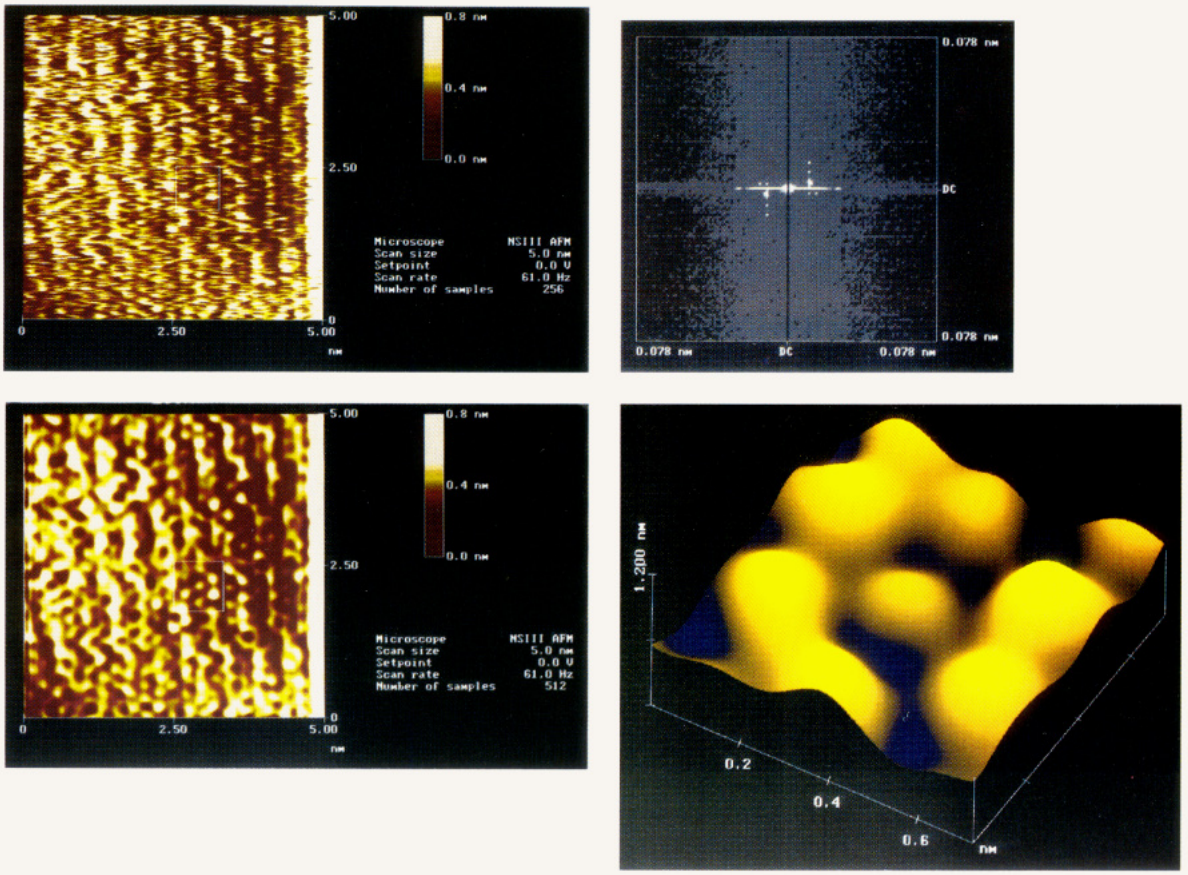

Figure 4. AFM images of a thermally treated Li-muscovite mica basal plane: (a, top left) a 5 nm × 5 nm unfiltered top view image; (b, top right) the 2-D fast Fourier transform of this raw image; (c, bottom left) a 5 nm high frequency filtered image; (d, bottom right) a three-dimensional surface image of the hexagonal array highlighted in (a) and (c) showing the Li^+ ion surrounded by six oxygen ions.

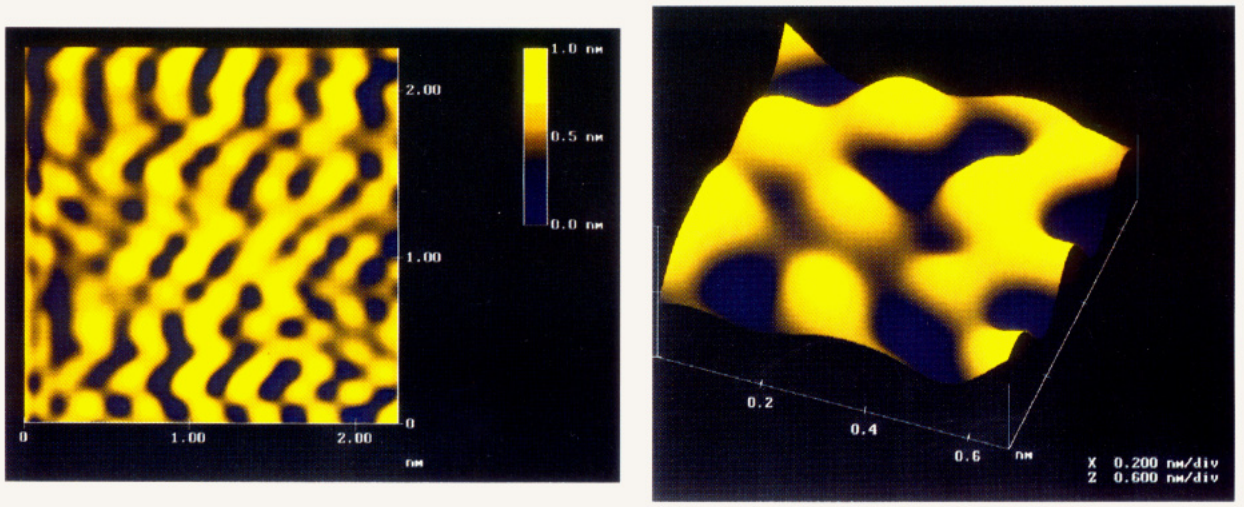

Figure 5. AFM images of a Mg-muscovite mica basal plane: (a, top) a 2 nm × 2 nm high frequency filtered top view image; (b, bottom) a three-dimensional surface image of a hexagonal array showing the Mg^{2+} ion surrounded by six oxygen ions.

In Figure 2c the image presented in Figure 2a is shown after high-frequency filtering of the data. The array of hexagonal rings of oxygens surrounding a vacant hexagonal hole can easily be seen. Finally, in Figure 2d we present a 3 nm × 3 nm close-up of some of the hexagons described in the previous images. Previous crystallographic studies of the mica basal plane have suggested that the ideal hexagonal array of oxygen ions must show some distortion due to a misfit between the tetrahedral and octahedral layers.[6] In this close-up image, one of the hexagons shows a clear shape distortion correspondent to such a misfit in the lattice. The center to center distance between the hexagonal holes in these images is 5.1 Å (±0.2 Å) while the nearest neighbor distance for each oxygen ion is 2.6−2.8 Å. In both cases these distances are, within experimental error, the expected dimensions from Figure 1.

A top-view image of K-mica is shown in Figure 3a. Once again, a regular array of light spots is also observed. Rows of close-packed spots can be observed along the arrow in Figure 3a. They are aligned with an inner spacing between them of 2.6−2.8 Å which is close to the theoretical diameter of a hexagonal cavity. A section analysis of the row of close-packed light spots in Figure 3b suggests that the center-to-center distances between neighboring spots in the rows give values of 2.4−2.6 Å which are almost the

diameter of a single oxygen atom. In addition, faint spots between the rows of close-packed spots are observed at a neighboring distance of about 5.2–5.7 Å as confirmed in a section analysis of Figure 3c. Hence, we can clearly indicate that the observed molecular pattern corresponds to the shaded rows of oxygen ions in Figure 3d. Each observed spot will correspond to either one, two, or three oxygens. This is also consistent with the image of Figure 3a in that some spots are seen to be locally separated into two or three smaller units.

In Figures 2 and 3, the number of oxygen ions per spot are not necessarily consistent even though regular arrays of the light spots and cavities could be observed. This may be due to the shape of the scanning tip in the AFM which cannot be controlled at the atomic level. The aspect of the tip atoms to those of the surface while imaging may also cause variations in the observed arrays if in certain scan directions different numbers of tip atoms contribute to the scanning interaction. We could not find any spots corresponding to interlayer cations such as K^+ ions which were expected to sit in the hexagonal cavities of the K^+-mica crystal structure. Hartman et al.[23] have also reported that they were unable to observe the interlayer cations on the basal plane of other 2:1-type clay minerals such as montmorillonite and illite. A possible explanation for this may be that the scanning tip displaces any ions weakly bound to the mica; alternatively K^+ ions might be released from the surface when the exchanged heat-treated mica was washed with water. In either case, the H- and K-micas have the same surface structure as the freshly cleaved muscovite mica basal plane during AFM scanning. In particular, the vacant hexagonal cavities are observed in all H- and K-micas when scanned with the AFM.

In Figure 4a, an unfiltered top-view image of the Li-mica shows a complicated and disordered array of light spots, unlike the H- and K-mica cases. In Figure 4b we show the 2-D Fourier transform of the data. The ordering of the data is again apparent for this system, although it is clear from this transformed data that the ordering is not as symmetrical as for the H- or K-mica samples. For clarity, the high-frequency filtered image of this array is given in Figure 4c. The regular array of the cavity surrounded by the light spots is no longer observed. The hexagonal rings of spots are again present, although in some cases a small central spot in the ring can also be observed. This is quite different from the H- and K-mica cases where no central spot in the cavity was observed.

A three-dimensional image for one of the typical hexagonal arrays of light spots is given in Figure 4d. The nearest center-to-center distance between the large spots of the hexagonal ring ranges from 2.5 to 2.6 Å. These values are very close to the theoretical nearest neighbor distance between the oxygens of the mica basal plane. The diameter of these spots is about 2.7 Å, which approximates to the diameter of the oxygen ions on the mica basal plane. The diameter of the central spots ranged from 1.4 to 1.6 Å. This is close to the effective packing diameter of 1.36 Å for a Li^+ ion.[24] We conclude that the large and small spots may be attributed to the oxygen and Li^+ ions, respectively.

As shown in Figure 5a, a high-frequency filtered top-view image of the Mg-mica also shows an irregular array of the light spots although they are not as well defined as the image of the Li-mica.

An enlarged, three-dimensional image of a hexagonal array of light spots in Figure 5b indicates that a central spot in the hexagon of the large spots is also observed as for the Li-mica case. The nearest center-to-center distance between the large spots of the hexagonal array and their respective diameters is 2.6 Å. The diameter of the central spots is approximately 1.4 Å, which is consistent with the effective packing diameter for a Mg^{2+} ion.[24] These observations imply that the large and the small spots can again be attributed to the oxygen and the Mg^{2+} ions, respectively.

Table 1. Zeta Potential of Freshly Cleaved and Heated Muscovite Mica Basal Planes (pH 5.3–5.8; Background Electrolyte 0.001 mol dm^{-3} LiCl)

sample	zeta potential, mV
freshly cleaved mica	−112 ± 5
treated micas	
H-mica	−110 ± 5
K-mica	−110 ± 5
Li-mica	−66 ± 5
Mg-mica	−68 ± 5

There is much controversy concerning the position of Li^+ and Mg^{2+} ions which are irreversibly fixed in 2:1 type sheet silicates. According to the concept invoked by Hofmann and Klemen[9] and Green-Kelly,[10,11] Li^+ and Mg^{2+} ions could migrate into a vacant site in the octahedral layer of a smectite, whereas Tettenhorst[25] concluded from IR spectra of heated Li-montmorillonite that Li^+ ions penetrate the Si–O network but not into the octahedral layer. Farmer and Russel[26] presented IR data indicating that Li^+ ions do not become fixed in the octahedral sites but react with structural hydroxyl groups to release protons. More recently, Jaynes and Bigham[27] indicated the cation-exchange capacity (CEC), which is closely related to the surface charge, decreases with increasing the octahedral charge in the dioctahedral smectites. The fixation of Li^+ ions in dioctahedral smectites which has mainly tetrahedral charge might be due to deprotonation of hydroxy group of the octahedral layer below the hexagonal cavity. Hence, it was not surprising that Li^+ and Mg^{2+} ions could be fixed in the hexagonal cavity of the muscovite mica given that muscovite is similar to the dioctahedral smectites with tetrahedral charge. If the fixation of Li^+ and Mg^{2+} ions actually occurs on the mica basal plan, the reduction in surface charge can be expected to be similar to the CEC reduction in Li-smectite reported by Jaynes and Bigham.[27] Accordingly, zeta potential measurements of the mica basal plane were conducted with an intention of testing change in the charge of the basal plane due to Li^+, Mg^{2+} fixation.

The zeta potential of the same mica basal plane as in the AFM observations was measured at pH 5.3–5.8 in the presence of 0.001 mol dm^{-3} LiCl. The zeta potential of H- and K-mica basal planes gave identical values to the freshly cleaved mica basal plane, while the zeta potential of Li- and Mg-mica basal planes was significantly reduced in magnitude. This result is consistent with the AFM images in that the spots could be observed in the hexagonal cavity on the Li- and Mg-micas, while no such spots were observed in the cavities for the K- and H-micas. The reduction in zeta potential of Li- and Mg-mica is therefore consistant with a reduction in the negative charge of the micas by Li^+ and Mg^{2+} ions which were irreversibly fixed in hexagonal cavities on the mica basal planes.

The difference in the AFM image and the magnitude of zeta potential depends markedly on the size of the dehydrated cations and that of the hexagonal hole as shown in the schematic diagrams of Figure 6: (1) in

(23) Hartman, H.; Sposito, G.; Yang, A.; Manne, S.; Gould, S. A. C.; Hansma, P. K. *Clays Clay Miner.* **1990**, *38*, 337.
(24) Israelachvili, J. N. *Intermolecular & Surface Forces*, 2nd ed.; Academic Press: London 1991; 110 pp.
(25) Tettenhorst, R. *Am. Mineral.* **1962**, *47*, 769.
(26) Farmer, V. C.; Russell, J. D. *Clays Clay Miner.* **1967**, *15*, 121.
(27) Jaynes, W. F.; Bigham, J. M. *Clays Clay Miner.* **1987**, *35*, 440.

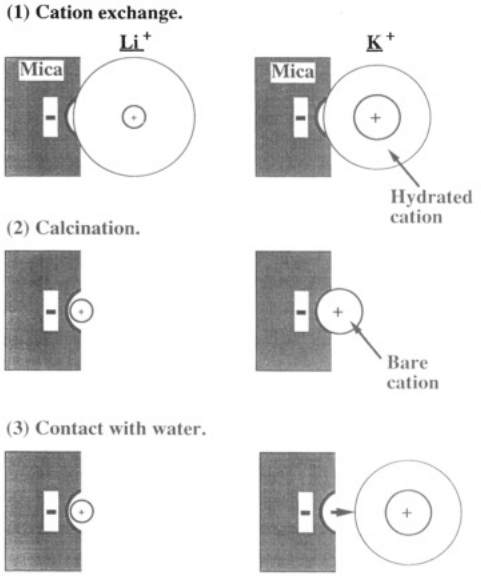

Figure 6. Schematic representation for the difference in fixation mechanisms of K^+ and Li^+ ions on a muscovite mica basal plane.

Table 2. Air–Water Contact Angles for Freshly Cleaved and Treated Muscovite Mica Basal Planes (Angle through Distilled Water Drop)

sample	contact angle, deg
freshly cleaved mica	<10
treated micas	
H-mica	30–35
K-mica	30–35
Li-mica	10–15
Mg-mica	10–20

electrolyte solution, the mica basal planes are equilibrated with hydrated cations approaching electrostatically to the hexagonal rings of oxygen atoms; (2) the cations on the hexagonal rings are dehydrated after heating, and the Li^+ ion, which is smaller in size than the hexagonal cavity, is able to enter the hexagonal ring, whereas K^+ ion does not; (3) when the mica basal planes contact water, Li^+ ion can still be retained in the cavity, while the K^+ ion is rehydrated and released to water. This argument supports that the fixation of inorganic cations on the 2:1 type silicates depends on whether dehydrated cations are able to enter hexagonal cavities of the molecular network on the basal plane.

The contact angle results shown in Table 2 provide important additional information. Here a drop of pure water is placed on the freshly cleaved or heat-treated mica samples. The freshly cleaved untreated sample yields a low contact angle indicating almost complete spreading of the drop on this surface. In contrast the thermally treated H- and K-mica samples show a significantly higher, i.e., partially nonwetting angle. Finally, the Li- and Mg-treated micas show a near zero wetting condition.

These results indicate that the H- and K-micas, which do not contain cations locked in the hexagonal hole, have suffered some loss of hydrophilic character. Without cations in place, as in the freshly cleaved case, hydration sites are minimal. There may be some annealing out of strain in the sheet which again will minimize higher energy hydratable sites. Finally, for the Li and Mg cases there must be some tendency for water to react with the buried cations, without releasing them, and complete wetting is observed.

Conclusion

The AFM images of exchanged and heat-treated H- and K-mica reflected the ideal array of oxygen ions which was almost identical to the known arrangement of the fresh cleaved basal plane. No ions were observed in the hexagonal cavity surrounded by oxygen atoms. The image of H-mica which corresponds to a bare basal plane where no interlayer cation exists substantiated that the calcination would not damage the molecular pattern of the basal plane. The images of Li- and Mg-micas showed a significant irregular array of oxygen ions on the basal planes and small spots other than oxygen ions in the hexagonal cavity could be observed. Furthermore, the zeta potential of H- and K-mica basal planes showed identical values to the freshly cleaved mica basal plane, while the zeta potentials of Li- and Mg-mica basal planes were much lower in magnitude than that of freshly cleaved mica. These results suggest that Li^+ and Mg^{2+} ions were irreversibly fixed in the hexagonal cavity on the mica basal plane, resulting in a reduced negative charge. On the other hand, K^+ ions could not be fixed in the hexagonal cavity. Such cation fixation depends on whether the bare cations are able to enter the hexagonal cavities on the mica basal plane. Contact angle results for a drop of pure water on the freshly cleaved and heat-treated micas were consistant with these image and electrokinetics results.

Acknowledgment. S.N. would like to thank the Japanese government for providing a scientific research scholarship for travel and research at the University of Melbourne. The funding of the Advanced Mineral Products Special Research by the Australian Research Concil is gratefully acknowleged. We thank Professor J. P. Quirk of the University of Western Australia for helpful discussions.